The current issue and full text archive of this journal is available at
www.emeraldinsight.com/0332-1649.htm

Numerical modelling of non-linear coupled thermo-electric problems

A comparative study

Igor O. Golosnoy and Jan K. Sykulski
School of Electronics and Computer Science, University of Southampton, Southampton, UK

Abstract

Purpose – The purpose of this paper is to access performance of existing computational techniques to model strongly non-linear coupled thermo-electric problems.

Design/methodology/approach – A thermistor is studied as an example of a strongly non-linear diffusion problem. The temperature field and the current flow in the device are mutually coupled via ohmic heating and very rapid variations of electric conductivity with temperature and applied electric field, which makes the problem an ideal test case for the computational techniques. The finite volume fully coupled and fractional steps (splitting) approaches on a fixed computational grid are compared with a fully coupled front-fixing method. The algorithms' input parameters are verified by comparison with published experiments.

Findings – It was found that fully coupled methods are more effective for non-linear diffusion problems. The front fixing provides additional improvements in terms of accuracy and computational cost.

Originality/value – This paper for the first time compares in detail advantages and implementation complications of each method being applied to the coupled thermo-electric problems. Particular attention is paid to conservation properties of the algorithms and accurate solutions in the transition region with rapid changes in material properties.

Keywords Numerical analysis, Thermal diffusion, Thermoelectricity

Paper type Research paper

1. Introduction

A thermistor is a thermally sensitive resistor. Barium titanate ($BaTiO_3$) is a common material for use in thermistors due to its very non-linear dependence of electric conductivity σ on temperature T (Macklen, 1979). This property makes thermistors attractive in various applications such as temperature sensors, switching devices and current limiters.

The changes in σ are extremely large, typical variations of five orders of magnitude with T increasing from 100 to 200°C have been reported (Fowler *et al.*, 1992; Supancic, 2000) (Figure 1). While a ferroelectric-paraelectric phase transition takes place between temperatures T_1 and T_2, the physical transition region between space coordinates s_1 and s_2 is typically small and a coupled treatment of electric and thermal fields is complex. Earlier studies ignored the transition and considered a sharp interface with a step behaviour in σ (Chen and Friedman, 1993; Westbrook, 1989; Wood and Kutluay, 1995). But it was noted (Fowler *et al.*, 1992) that the step function is not the most realistic model for σ and that a more complex $\sigma(T)$ should be used for accurate predictions. A dependence of σ (Preis *et al.*, 1994; Supancic, 2000) and dielectric constant ε (Preis *et al.*, 2003) on electric field E across the device is an additional complication in the formulation.

COMPEL: The International Journal for Computation and Mathematics in Electrical and Electronic Engineering
Vol. 28 No. 3, 2009
pp. 639-655

0332-1649
DOI 10.1108/03321640910940909

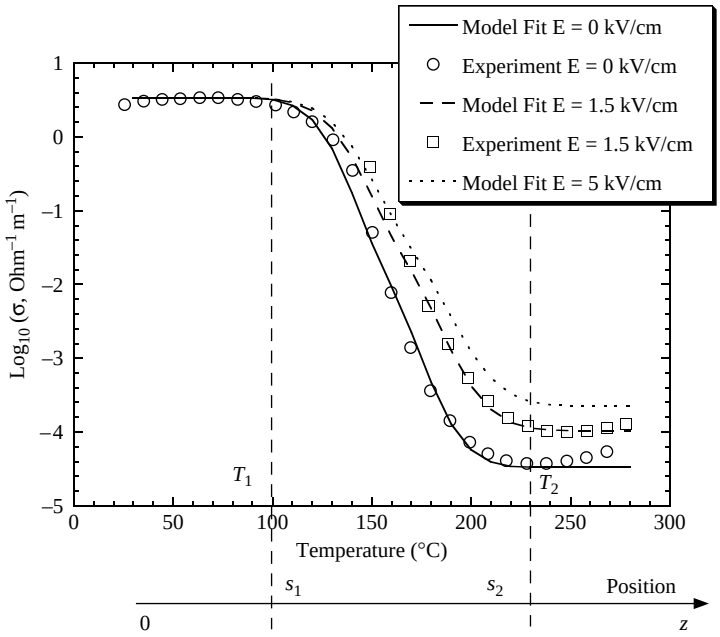

Figure 1.
Typical variation of electric conductivity with temperature for a $BaTiO_3$ thermistor

Notes: Measured conductivity at different field strength (Supancic, 2000) is fitted by interpolation described in the Appendix

Numerical simulations are required to describe accurately the electrical behaviour of the thermistor and to predict temperature profiles in the device together with thermal stresses. Numerical solutions of such coupled non-linear thermo-electric problems encounter difficulties with limitations on time step for explicit methods (Wood and Kutluay, 1995), non-physical oscillations (Kutluay *et al.*, 1999) and iterations convergence (Preis *et al.*, 1994, 2003). One could expect that fully implicit schemes should provide very reliable algorithms, even if they are only first order accurate in time. But extreme variation in $\sigma(T)$ in a very short time necessitates introduction of a significant under-relaxation factor (0.05-0.3) in the iterations (Preis *et al.*, 1994, 2003), which of course slows down the convergence. It could be argued that the convergence could be significantly improved by adaptive meshes which allow to dynamically arrange nodes in the transition region, but this is only effective for problems with weak non-linearity. In our case, a simple interpolation of the electric conductivity into new adapted positions results in violating the Poisson equation for electric potential. Careful interpolation might be possible but it would be accompanied by mathematical complications. Thus, the objective is for a numerical technique to adapt the nodes' positions automatically and, as a result, satisfy easily conservation laws.

This paper deals with modelling of a coupled electric current and heat flow in a thermistor with a particular attention paid to a moving transient region. The motion is assumed to be a complex function of the solution itself. Many numerical methods developed previously, such as front tracking or re-meshing techniques (Crank, 1984), are often not able to cope effectively with such a strong coupling. On the other hand, the front-fixing transformations (Crank, 1984) introduce a co-ordinate system in which

all of the spatial region boundaries are fixed to s_1 and s_2. One advantage of discretising in the transformed space is that the meshes automatically adjust themselves to accommodate the moving interface position. It is therefore possible to impose irregular meshes with fine resolution in regions where large temperature and field gradients are expected, while using larger space steps elsewhere. (Such approach has already been shown to be very effective in modelling an electric field penetration into high-temperature superconducting tapes (Golosnoy and Sykulski, 2008).) The main challenge is a consistent implementation of conservation laws with the phase boundaries motion and an effective positioning of the nodes. These issues are addressed in the paper.

2. Formulation of the problem

2.1 Geometry of the device and material properties

Typically, the device is a ceramic disk with a diameter r_{ext} of about 3-10 mm and thickness ($2\ z_{ext}$) of about 2 mm with a wire soldered to the flat edges (Fowler *et al.*, 1992; Supancic, 2000; Preis *et al.*, 2003). For the modelling tests presented here, $r_{ext} = 1.5$ mm, $z_{ext} = 1.25$ mm were chosen (Figure 2).

The material properties used for the modelling are similar to those given in Supancic (2000) and they are listed in Table I. To simplify the modelling, a continuous interpolation for conductivity σ values for different temperature T and electric field E has been developed. The main objective of the paper is to assess computational performance of various numerical techniques. For this reason, the interpolation should provide qualitative description of the $\sigma(T, E)$, while perfect agreement with experimental values would not be expected. Details of the interpolation procedure are given in the Appendix.

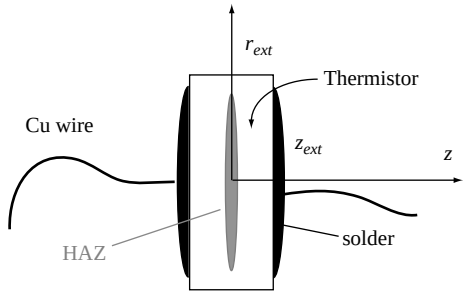

Figure 2.
Geometry of the thermistor device

Property	Symbol (units)	Value
Thermal conductivity	κ (W m^{-1}K^{-1})	2.5
Specific heat	C (J kg^{-1}K^{-1})	500
Density	ρ (kg m^{-3})	5,660
Electric conductivity at room temperature	σ_1 (Ω^{-1}m^{-1})	3.33
Electric conductivity at high temperature (low-electric field)	σ_2 (Ω^{-1}m^{-1})	3.33×10^{-5}
Boundary of high-conductive phase	T_1 (K)	90
Boundary of low-conductive phase	T_2 (K)	230

Table I.
Material properties

2.2 Electric circuit and governing equations

$BaTiO_3$ has abnormally high-electric permittivity (relative values of several thousand have been reported (Preis *et al.*, 2003)) and displacement currents could influence the electric potential even at relatively low frequencies, should the value of the displacement current become comparable to the transport (conduction) current. Experiments (Preis *et al.*, 2003) suggest that the dielectric effects become important if transport current densities drop below a few Am^{-2} at 50 Hz. However, the paper considers values of J of thousands Am^{-2}, and under such conditions the displacement current is negligible. The electric current flow in the system and associated Joule heating are then well described by standard Ohm's law:

$$\nabla \mathbf{J} = 0, \quad \mathbf{J} = \sigma \nabla \phi, \quad Q_{el} = \sigma^{-1}\mathbf{J}^2 = \sigma(\nabla\phi)^2, \tag{1}$$

where $\mathbf{J}$ is the current density, ϕ is an electric potential, Q_{el} is a Joule heat. For simplicity, the electric circuit includes external voltage V_0 applied to a load R_0 in series with the thermistor.

When a high current passes through the thermistor, Joule heat is released in the middle of the device. The heat-affected zone with low conductivity develops inside the thermistor. It has initially a complex shape but for $r_{ext} \gg z_{ext}$ it almost immediately spreads to the edges, the transformation front becomes straight and the problem can be approached using a 1D approximation with all parameters dependent on the z-coordinate only. The current density is linked with the external load and the variable conductivity inside the device:

$$V_0 = J\left(\pi r_{ext}^2 R_0 + 2\int_0^{z_{ext}} \frac{dz}{\sigma(T)}\right), \tag{2}$$

This is coupled with the heat transport which is governed by the heat-diffusion equation:

$$C\rho \frac{\partial T}{\partial t} = \frac{\partial}{\partial z}\left(\kappa \frac{\partial}{\partial z} T\right) + \sigma^{-1}J^2, \tag{3}$$

where C is the specific heat, ρ is the density, and κ is the thermal conductivity. Since a dependence of $C\rho$ on temperature can be removed by integral transformation (Carlslaw and Jaegar, 1959), the $C\rho$ has been assumed to be constant for simplicity. Appropriate initial and boundary conditions for equations (1)-(3) are discussed elsewhere (Fowler *et al.*, 1992). For example, the heat losses from the edges $z = \pm z_{ext}$ are modelled using effective heat transfer coefficient $h_{ext} = 1{,}200\ \mathrm{W\,m^{-2}K^{-1}}$ and environmental temperature $T_{ext} = 24\,^{\circ}\mathrm{C}$, whereas heat losses at $r = r_{ext}$ are ignored. Such high value of h_{ext} represents a combined effect of air convection and heat taken away by copper wires and solder (Fowler *et al.*, 1992; Supancic, 2000). Heat flux at $z = 0$ is assumed to be zero due to the problem symmetry. Initially, the temperature is uniform across the device $T(z,\ t = 0) = 24\,^{\circ}\mathrm{C}$. Electric potential at $z = \pm z_{ext}$ is implicitly defined by the circuit equation (2) and Ohm's law (equation (1)). For field dependent $\sigma(T, E)$, equations (1) and (2) must be solved by iterations. In the above form, equations (1)-(3) provide an excellent case for testing various numerical techniques to solve coupled thermo-electric diffusion problems.

3. Numerical modelling techniques

3.1 Fixed grid

Second order approximations in both space and time require semi-implicit finite volume approximation for equation (3) (Tannehill *et al.*, 1997). Integrals of equation (3) around each node i over one-time step Δt provide a set of conservative equations in the bulk material (LeVeque, 2002), which are represented on a fixed grid by equation (4), where a subscript notation to denote discretisations of space (e.g. z_i, $z_0 = 0$, $z_M = z_{ext}$) is used and superscripts (e.g. t^j) indicate time:

$$\left(T_i^{j+1} - T_i^j\right)(z_{i+0.5} - z_{i-0.5}) = (t^{j+1} - t^j)\left(\frac{\kappa_{i+0.5}}{C\rho}\frac{T_{i+1}^{j+0.5} - T_i^{j+0.5}}{z_{i+1} - z_i} - \frac{\kappa_{i-0.5}}{C\rho}\frac{T_i^{j+0.5} - T_{i-1}^{j+0.5}}{z_i - z_{i-1}}\right) + (t^{j+1} - t^j)\frac{(z_{i+0.5} - z_{i-0.5})}{2C\rho}\left(\frac{\left(J_i^j\right)^2}{\sigma_i^j} + \frac{\left(J_i^{j+1}\right)^2}{\sigma_i^{j+1}}\right), \tag{4}$$

where κ could depend on T, and $T_i^{j+0.5} = 0.5(T_i^{j+1} + T_i^j)$. Neumann boundary conditions for equation (4) are approximated in a standard manner to keep the second-order accuracy in space on a uniform grid (Tannehill *et al.*, 1997), e.g. at $z_M = z_{ext}$:

$$\left(T_M^{j+1} - T_M^j\right)(z_M - z_{M-0.5}) = (t^{j+1} - t^j)\left(\frac{h_{ext}}{C\rho}\left(T_{ext} - T_M^{j+0.5}\right) - \frac{\kappa_{M-0.5}}{C\rho}\frac{T_M^{j+0.5} - T_{M-1}^{j+0.5}}{z_M - z_{M-1}}\right) + (t^{j+1} - t^j)\frac{(z_M - z_{M-0.5})}{C\rho}\left(\frac{\left(J_M^j\right)^2}{\sigma_M^j} + \frac{\left(J_M^{j+1}\right)^2}{\sigma_M^{j+1}}\right). \tag{5}$$

The conductivity σ and the Joule heat source in equation (4) are very sensitive to temperature variation and they should be estimated at the grid point. That is why the current density is defined by approximating the potential equation (1) on a staggered grid, which yields:

$$\frac{1}{z_{i+1} - z_i}\left(J_{i+1}^{j+1} - J_i^{j+1}\right) = 0, \quad J_i^{j+1} = \sigma_i\left(T_i^{j+1}, E_i^{j+1}\right)\cdot E_i^{j+1}, \quad E_i^{j+1} = \frac{\phi_{i+0.5}^{j+1} - \phi_{i-0.5}^{j+1}}{z_{i+0.5} - z_{i-0.5}}, \tag{6}$$

with identical boundary conditions at $i = 0$, $i = M$, e.g.:

$$J_0^{j+1} = \sigma_0(T_0, E_0)\cdot E_0^{j+1}, \quad E_0^{j+1} = \frac{\phi_{0.5}^{j+1} - \phi_0^{j+1}}{z_{0.5} - z_0} \tag{7}$$

and the circuit equation:

$$V_0 = \pi r_{ext}^2 J_M^{j+1} R_0 + 2\left(\phi_M^{j+1} - \phi_0^{j+1}\right). \tag{8}$$

In fact, equations (6)-(8) are reduced to a set of resistances in series for the 1D problem where $J(z, t) \equiv J(t)$ only. Since all of the equations are coupled, the entire system (equations (4)-(8)) must be solved simultaneously. They form a non-linear system and this is potentially very demanding in terms of computing times. It is suggested to introduce two enclosed iteration cycles to solve the system effectively. In the internal cycle, equations (6)-(8) are solved for a given estimate of the temperature field. On each step the previous estimate for $\sigma(T, E^{j+1})$ is used with iterations (p) continuing until:

$$\left| 1 - \frac{{}^{(p+1)}J_M^{j+1}}{{}^{(p)}J_M^{j+1}} \right| \geq 10^{-2}.$$

This provides an update for the heat source in equations (4)-(5) which are inverted on each external iteration cycle using the Thomas tridiagonal algorithm. External iteration cycles (k) continue until:

$$\max_i \left| 1 - \frac{{}^{(k+1)}T_i^{j+1}}{{}^{(k)}T_i^{j+1}} \right| \geq 10^{-4}.$$

Normally, it takes only two iterations to reach a consistent solution of a fully coupled sets (4) and (5) under smooth operation conditions, whereas modelling of the temperature surge event could require as many as 10 or even 20 iterations.

3.2 Fractional steps method

It is a common computational practice to separate source terms from the diffusion. The so-called "fractional steps" or "splitting methods" are widely used in computational fluid dynamic for modelling of gas flow with chemical reactions (Tannehill *et al.*, 1997; LeVeque, 2002). On the first sub-step only diffusional fluxes in equation (4) contribute to temperature changes in a cell:

$$\left(\tilde{T}_i^{j+1} - T_i^j\right)(z_{i+0.5} - z_{i-0.5}) = (t^{j+1} - t^j)\left(\frac{\kappa_{i+0.5}}{C\rho}\,\frac{\tilde{T}_{i+1}^{j+0.5} - \tilde{T}_i^{j+0.5}}{z_{i+1} - z_i} - \frac{\kappa_{i-0.5}}{C\rho}\,\frac{\tilde{T}_i^{j+0.5} - \tilde{T}_{i-1}^{j+0.5}}{z_i - z_{i-1}}\right) \tag{9}$$

Joule heat sources in equation (4) are added during the second sub-step, which is effectively the second order Runge-Kutta integration:

$$\left(T_i^{j+0.5} - \tilde{T}_i^{j+1}\right) = \frac{(t^{j+0.5} - t^j)}{C\rho}\,\frac{\left(\tilde{J}_i^{j+1}\right)^2}{\tilde{\sigma}_i^j},$$

$$\left(T_i^{j+1} - \tilde{T}_i^{j+1}\right) = \frac{(t^{j+1} - t^j)}{C\rho}\,\frac{\left(J_i^{j+0.5}\right)^2}{\sigma_i^{j+0.5}}, \tag{10}$$

with current density obeying equations (6)-(8). The splitting makes the solution of the heat-diffusion part (equation (9)) free from iterations, but internal iterations for

equations (6)-(8) to find consistent current density and conductivities remain. It also requires small time steps for high accuracy to be achieved (Figure 6). This is not surprising since large changes in the temperature profile at the surge stage (Figure 5) due to Joule heat are directly influenced by strong thermal diffusion.

3.3 Front-fixing method

Landau transformation utilises new positional variables (one for each domain). In practical applications, the temperature rarely exceeds T_2. Only two domains with a boundary at $s = s_1$ need to be considered, constituting an additional simplification. In the plane case, an introduction of $u = z/s(t)$ fixes the extent of low-conductivity region A to the domain $0 \le u \le 1$, while $v = (z - s)/(z_{ext} - s)$ fixes the extent of the other domain B to $0 \le v \le 1$ (Crank, 1984). Using the results from Illingworth and Golosnoy (2005), the conservative form of equation (3) for u and v together with equation (1) for potential and interface equations at s may be written as:

$$\frac{\partial(C\rho sT)}{\partial t} = \frac{ds}{dt}\frac{\partial(C\rho uT)}{\partial u} + \frac{1}{s}\frac{\partial}{\partial u}\left(\kappa\frac{\partial T}{\partial u}\right) + s\sigma\left(\frac{\partial\phi}{\partial u}\right)^2, \tag{11}$$

$$\frac{\partial(C\rho(z_{ext}-s)T)}{\partial t} = \frac{ds}{dt}\frac{\partial(C\rho(1-v)T)}{\partial v} + \frac{1}{(z_{ext}-s)}\frac{\partial}{\partial v}\left(\kappa\frac{\partial T}{\partial v}\right) + (z_{ext}-s)\sigma\left(\frac{\partial\phi}{\partial v}\right)^2 \tag{12}$$

$$\frac{\partial}{\partial u}\left(\sigma\frac{\partial\phi}{\partial u}\right) = 0, \quad u \in (0,1); \quad \frac{\partial}{\partial v}\left(\sigma\frac{\partial\phi}{\partial v}\right) = 0, \quad v \in (0,1); \tag{13}$$

with additional interface conditions for temperature and potential:

$$\frac{1}{s}\left(\kappa\frac{\partial T}{\partial u}\right)\Bigg|_{u=1} = \frac{1}{z_{ext}-s}\left(\kappa\frac{\partial T}{\partial v}\right)\Bigg|_{v=0}, \tag{14}$$

$$\frac{1}{s}\left(\sigma\frac{\partial\phi}{\partial u}\right)\Bigg|_{u=1} = \frac{1}{z_{ext}-s}\left(\sigma\frac{\partial\phi}{\partial v}\right)\Bigg|_{v=0}. \tag{15}$$

It should be noted that the Landau transformation introduces a co-ordinate system in which all of the spatial boundaries are fixed to 0 or 1. Under the transformation, the new computational domains remain the same with an additional advection term in equations (11) and (12) and implicit non-linear equations for the boundary motion (equations (14) and (15)). This allows treating the nodes close to the interface as being independent of the motion, which gives higher accuracy for the same number of nodes used. A divergent form of equations (11)-(15) ensures that there are no artificial energy sources (Illingworth and Golosnoy, 2005).

Equations (11)-(15) represent a typical Stefan problem with the so-called implicit moving boundary (Crank, 1984) and strongly non-linear Joule heat source. The interface position is not strictly defined in this case and the displacement of s should be selected from physical considerations. The "effective" transformation temperature T_1 can be varied during the modelling in such a way so as to achieve better description of the transient process.

Modelling of high thermo-mechanical stresses in thermistors involves a 2D simulation of the temperature distribution at the initial surge stage (Preis *et al.*, 1994, 2003).

The front-fixing technique allows an easy extension to 2D geometry as shown in Crank (1984). The resulting set of the differential equations is similar to equations (11) and (12) and it can be solved by the numerical method described below.

Numerical scheme. In order to derive a finite volume scheme, space is discretised at $M+1$ points. The first $N+1$ points are defined by a fixed discretisation of u, which corresponds to the extent of A. The points in A are written as $u_0 = 0,\ u_1, \ldots, u_N = 1$. The last $M-N+1$ points are in B as given by a fixed discretisation $v_N = 0,\ v_{N+1}, \ldots, v_M = 1$. The finite volume discretisation (LeVeque, 2002) of equations (11) and (12) is based on integration around the nodes and is fairly straightforward (Illingworth and Golosnoy, 2005), e.g. for the high-temperature phase A:

$$\begin{aligned}
&\left(T_i^{j+1}s^{j+1} - T_i^j s^j\right)(u_{i+0.5} - u_{i-0.5}) \\
&\quad = (s^{j+1} - s^j)\left(\frac{T_{i+1}^{j+0.5} + T_i^{j+0.5}}{2}\,u_{i+0.5} - \frac{T_i^{j+0.5} + T_{i-1}^{j+0.5}}{2}\,u_{i-0.5}\right) \\
&\qquad + \frac{t^{j+1} - t^j}{C\rho s^{j+0.5}}\left(\kappa_{i+0.5}\frac{T_{i+1}^{j+0.5} - T_i^{j+0.5}}{u_{i+1} - u_i} - \kappa_{i-0.5}\frac{T_i^{j+0.5} - T_{i-1}^{j+0.5}}{u_i - u_{i-1}}\right) \\
&\qquad + \frac{t^{j+1} - t^j}{2C\rho}(u_{i+0.5} - u_{i-0.5})\left(s^j\frac{\left(J_i^j\right)^2}{\sigma_i^j} + s^{j+1}\frac{\left(J_i^{j+1}\right)^2}{\sigma_i^{j+1}}\right),
\end{aligned} \tag{16}$$

with short notations:

$$\frac{T_{i+1}^{j+0.5} - T_i^{j+0.5}}{s^{j+0.5}} \equiv \frac{1}{2}\left(\frac{T_{i+1}^j - T_i^j}{s^j} + \frac{T_{i+1}^{j+1} - T_i^{j+1}}{s^{j+1}}\right), \quad T_i^{j+0.5} = 0.5\left(T_i^{j+1} + T_i^j\right) \tag{17}$$

Boundary conditions are approximated by noting that $u_0 = 0,\ 1 - v_M = 0$, e.g. for equation (5):

$$\begin{aligned}
&\left(T_M^{j+1}\left(z_{ext} - s^{j+1}\right) - T_M^j\left(z_{ext} - s^j\right)\right)(v_M - v_{M-0.5}) \\
&\quad = \left(s^{j+1} - s^j\right)\left(0 - \frac{T_{M-1}^{j+0.5} + T_M^{j+0.5}}{2}(1 - v_{M-0.5})\right) \\
&\qquad + \left(t^{j+1} - t^j\right)\left(\frac{h_{ext}}{C\rho}\left(T_{ext} - T_M^{j+0.5}\right) - \frac{\kappa_{M-0.5}}{C\rho\left(z_{ext} - s^{j+0.5}\right)}\frac{\left(T_M^{j+0.5} - T_{M-1}^{j+0.5}\right)}{(v_M - v_{M-1})}\right) \\
&\qquad + \frac{t^{j+1} - t^j}{2C\rho}(v_M - v_{M-0.5})\left((z_{ext} - s^j)\frac{\left(J_M^j\right)^2}{\sigma_M^j} + (z_{ext} - s^{j+1})\frac{\left(J_M^{j+1}\right)^2}{\sigma_M^{j+1}}\right).
\end{aligned} \tag{18}$$

The interface equations are approximated in a consistent way to conserve energy (Illingworth and Golosnoy, 2005), e.g. for equation (14) ($h_u = u_N - u_{N-1} \equiv 1 - u_{N-1}$, $h_v = v_{N+1} - v_N \equiv v_{N+1}$):

$$\begin{aligned}
&\left(T_N^{j+1}s^{j+1} - T_N^j s^j\right)\frac{h_u}{2} + \left(T_N^{j+1}\left(z_{ext} - s^{j+1}\right) - T_N^j\left(z_{ext} - s^j\right)\right)\frac{h_v}{2} \\
&\quad = (s^{j+1} - s^j)\left(\frac{T_N^{j+0.5} + T_{N+1}^{j+0.5}}{2}(1 - v_{N+0.5}) - \frac{T_{N-1}^{j+0.5} + T_N^{j+0.5}}{2}u_{N-0.5}\right) \\
&\qquad + \frac{t^{j+1} - t^j}{C\rho}\left(\kappa_{N+0.5}\frac{T_{N+1}^{j+0.5} - T_N^{j+0.5}}{h_v(z_{ext} - s^{j+0.5})} - \kappa_{N-0.5}\frac{T_N^{j+0.5} - T_{N-1}^{j+0.5}}{h_u s^{j+0.5}}\right) \\
&\qquad + \frac{t^{j+1} - t^j}{2C\rho}\left(\left(s^j\frac{h_u}{2} + (z_{ext} - s^j)\frac{h_v}{2}\right)\frac{\left(J_N^j\right)^2}{\sigma_N^j}\right. \\
&\qquad \left. + \left(s^{j+1}\frac{h_u}{2} + (z_{ext} - s^{j+1})\frac{h_v}{2}\right)\frac{\left(J_N^{j+1}\right)^2}{\sigma_N^{j+1}}\right).
\end{aligned} \tag{19}$$

The interface position is defined implicitly by requiring that:

$$\begin{aligned}
&T_N^{j+1}(\text{at } s^{j+1}) = 0.666\left(T_0^{j+1} + T_M^{j+1}\right), \quad \text{if } 0.666\left(T_0^{j+1} + T_M^{j+1}\right) < 150℃, \\
&T_N^{j+1}(\text{at } s^{j+1}) = 150℃, \quad \text{if } 0.666\left(T_0^{j+1} + T_M^{j+1}\right) \geq 150℃.
\end{aligned} \tag{20}$$

The particular choice in equation (20) ensures that the grid nodes are adjusted to the crucial location in the centre of the thermistor. The equation for potentials (equation (13)) in the transformed space (u, v) has the structure identical to the physical coordinate system (z). It is discretised in a similar way to equations (6)-(8).

The set of the simultaneous equations (16)-(20) involves the unknown future temperature field and potentials together with the unknown future interface position. Since all of the equations are coupled, the entire system must be solved simultaneously in order to conserve energy. This is a non-linear system and the computing times could be high. It is interesting to note that equations (11), (12) and (14), as well as equations (13) and (15), are only weakly coupled; thus, if the future interface positions were known, the diffusion problem (equations (11) and (12)) would become quasi-linear. With a known temperature profile, the potential could be found from equations (13) and (15) using standard iteration algorithms. Conversely, if the future temperature and potentials were known, the future interface position could be calculated easily from equation (20). It is possible to derive an efficient algorithm based on de-coupling the problem in this way. It is suggested not to introduce an additional external iteration cycle over the interface position s^{j+1} to solve the system effectively. At the internal cycles (similar to fixed grid situation), both the value of the interface position s^{j+1} and the temperature T^{j+1} are fixed. The solution of the Poisson equation provides an estimate of current density J^{j+1}. Equations (16)-(19) become linear with respect to T^{j+1} in the external iteration cycle so that they can be quickly inverted by a tridiagonal algorithm. After the new solution of equations (16)-(19) is obtained, the interface position s^{j+1} is updated via equation (20). Iteration cycles (k) continue until:

$$\max_i \left| 1 - \frac{{}^{(k+1)}T_i^{j+1}}{{}^{(k)}T_i^{j+1}} \right| \geq 10^{-4}.$$

It has been found that the algorithm requires similar (or sometimes even a smaller) number of iterations to reach a consistent solution in comparison with those on a fixed grid.

The transformed equations (11) and (12) include an advection term on the right hand side. The effective velocity is proportional to the interface displacement and new coordinates u and $(1 - v)$. This velocity is large close to the interface $u = 1$ and the modelling could face problems with oscillations at the front. Such non-monotonic behaviour could be avoided by using up/down-wind approximation for the advection term (Illingworth and Golosnoy, 2005; Tannehill *et al.*, 1997), but this would decrease the order of space approximation. On the other hand, a reversible flux transport corrected algorithm (Boris and Book, 1976) provides reasonable second-order accuracy in space and time with only ~ 25 per cent increase in computational cost. In all cases studied here, the corrections are found to be small and the flux correction (Boris and Book, 1976) provides only a minor improvement.

4. Validation

A sensible choice of the modelling parameters has been guided and verified by comparisons of the model predictions with published experimental results of DC and AC switching processes in thermistors with $r_{ext} = 1.5\,\text{mm}$, $2\,z_{ext} = 2.5\,\text{mm}$ (Supancic, 2000). The agreement between theory and experiment is encouraging for the DC load (Figure 3(a)). Although the model underestimates the maximum current at the end of the AC switching (Figure 3(b)), it still captures correctly the transition point. Side cooling was neglected in the paper, but it is important for periodic loads since it decreases the temperature, gives rise to conductivity and slows down the temperature relaxation. Generally, Figure 3 appears to show that the input parameters were chosen within a correct range.

Thermography was used recently (Platzer *et al.*, 2006) for surface temperature measurements $T(r_{ext}, z)$ on thermistors with $r_{ext} = 10\,\text{mm}$, $2\,z_{ext} = 5\,\text{mm}$. Specific details of material properties are not provided in Platzer *et al.* (2006) but current history during switching suggests quite low conductivity. Values of $\sigma_1 = 0.53\,\Omega^{-1}\,\text{m}^{-1}$, $\sigma_2 = 8.4 \times 10^{-6}\,\Omega^{-1}\,\text{m}^{-1}$, $T_1 = 105\,\text{K}$ and $T_2 = 235\,\text{K}$ give good agreement with the current measurements reported (Platzer *et al.*, 2006). These values were therefore used to predict temperature profiles $T(z)$. The 1D model agrees well with the experiment at the central region but some noticeable bias exists at the corners $r = r_{ext}$, $z = z_{ext}$. This has been expected since the 1D model predicts temperature distribution deep inside the device ($r \sim 0$) whereas the measurements emphasize real 2D features of the process. But even the oversimplified 1D formulation captures well the moment of the surge event and the value of the temperature rise (Figure 4).

5. Temperature surge modelling

It is suggested to test the models at hostile conditions by enhancing the switching rates in the 300 V DC mode. Additional forced cooling was introduced into the model by increasing the heat exchange coefficient up to $h_{ext} = 3{,}000\,\text{W}\,\text{m}^{-2}\,\text{K}^{-1}$. The temperature in the thermistor initially starts to rise gradually when a high current passes through the circuit. It takes a fraction of a second to reach the low-conductivity

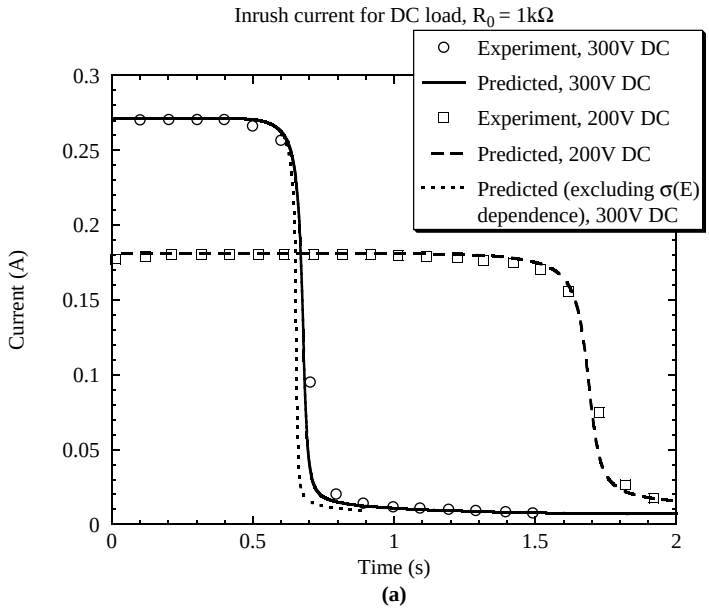

(a)

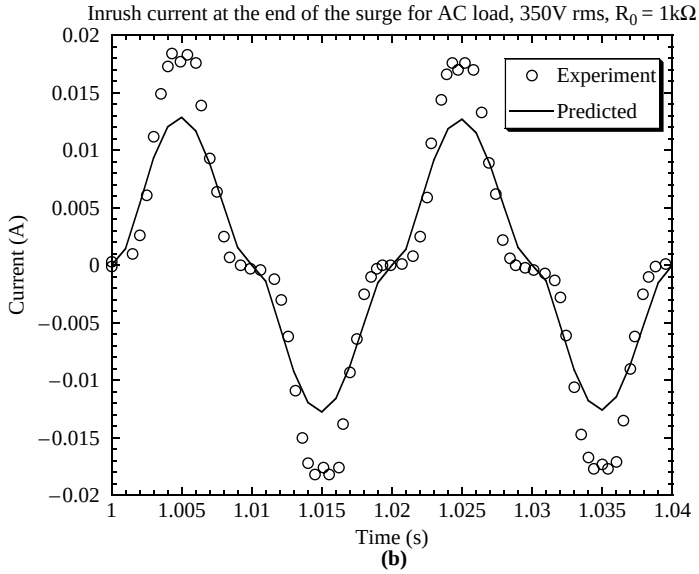

(b)

Notes: Test calculations were done on a fine uniform grid (100 intervals) with a small time step 0.1 ms

Figure 3.
Calculated and measured (Supancic, 2000) currents for: (a) DC and (b) AC load during temperature surge in a thermistor

phase (~120 °C) from the operational room temperature. At this stage, the surge takes place: the temperature increases by ~70 °C in 60 ms (Figure 5) and the current drops by an order of magnitude (Figure 6). Comparing the results with the field independent

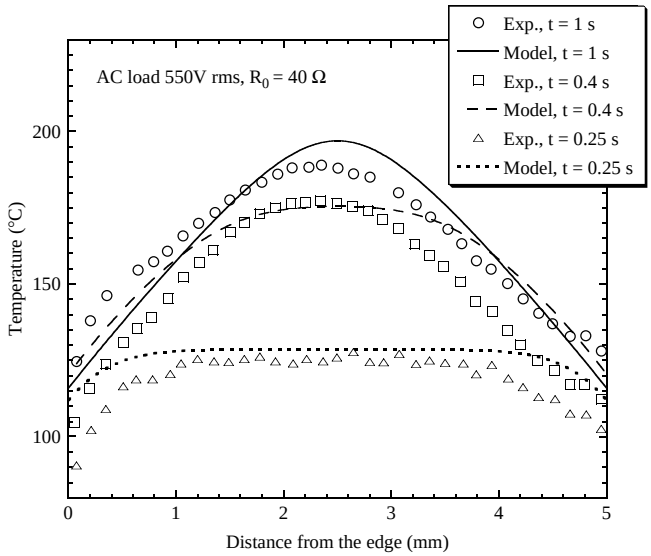

Figure 4.
Comparison of numerical predictions of temperature field in a thermistor at different time instants with surface thermography

Notes: Fully coupled formulation on fixed grid was used for the comparison. A mesh with 100 space intervals was applied and a time step of 0.2ms was taken
Source: Platzer *et al.* (2006)

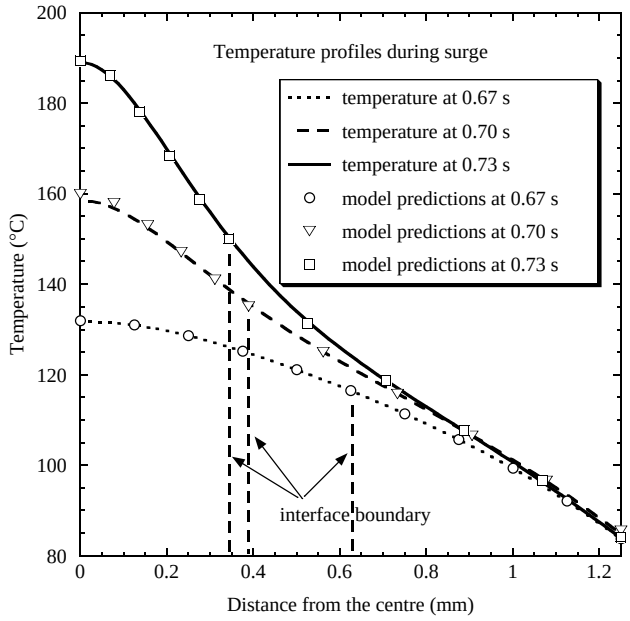

Figure 5.
Numerical predictions for temperature distribution in a thermistor at different time instants of the surge stage using the front-fixing technique

Notes: The nodes are automatically adjusted to high temperature region. Mesh with 10 space intervals was used and a time step of 10ms was taken. Benchmark temperature profiles were calculated on a fine uniform grid (100 intervals) with a small time step 0.1 ms

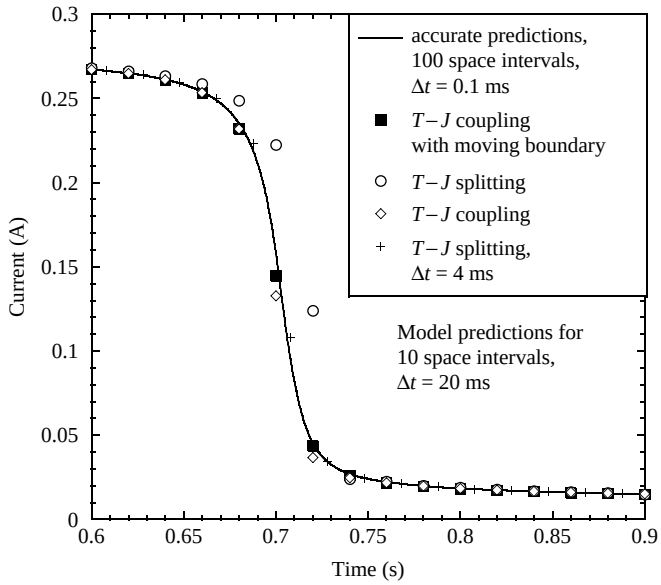

Figure 6.
Numerical predictions of current during temperature surge in a thermistor

case (Fowler *et al.*, 1992) (Figure 3(a)), it is clear that the switching is slowed down by dependence of conductivity on the electric field. This conclusion is in agreement with previous observations (Supancic, 2000).

It was found that a fully implicit, coupled scheme (Preis *et al.*, 2003) requires significant under-relaxation (~ 0.3) for iterations over the temperature field (equation (3)) to converge. The semi-implicit approximation used in this study has higher temporal accuracy. As a consequence, the scheme gives a better estimate of the temperature on the next time level and does not require under-relaxation for most cases. For example, a coupled fixed grid model needs under-relaxation only for $\Delta t > 40$ ms, whereas the front-fixing technique extends the limit up to $\Delta t > 50$ ms. But a major current drop occurs in 40 ms, between 0.68 and 0.72 s, and the reasonable time steps are now $\Delta t \sim$ 10-20 ms, which are well below the observed limits.

Looking at the predictions for the electric conductivity (Figure 7), it is obvious that conventional splitting methods fail to deliver sufficient accuracy during the surge at points with rapid temperature changes, as the method requires much smaller time steps to accomplish good accuracy (Figure 6). On the other hand, a fully coupled implicit method on a fixed grid provides reasonable accuracy for temperature and electric conductivity at most of the grid nodes (Figure 7). However, some errors still exist for predicted current density (Figure 6). This is related to the coarse discretisation at crucial locations (centre of the thermistor, $z = 0$) where the conductivity varies in an exponential manner. The current density is very sensitive to a detailed description of high-temperature (low-conductivity) regions and the nodes positions. That is why the adjustment of nodes to the crucial location by moving the coordinate system yields excellent accuracy even for large time steps and a small number of discretisation points.

Finally, as demonstrated in Table II, the splitting method could be time consuming for non-linear problems. Since Poisson equation with complex $\sigma(T, E)$ has to be solved

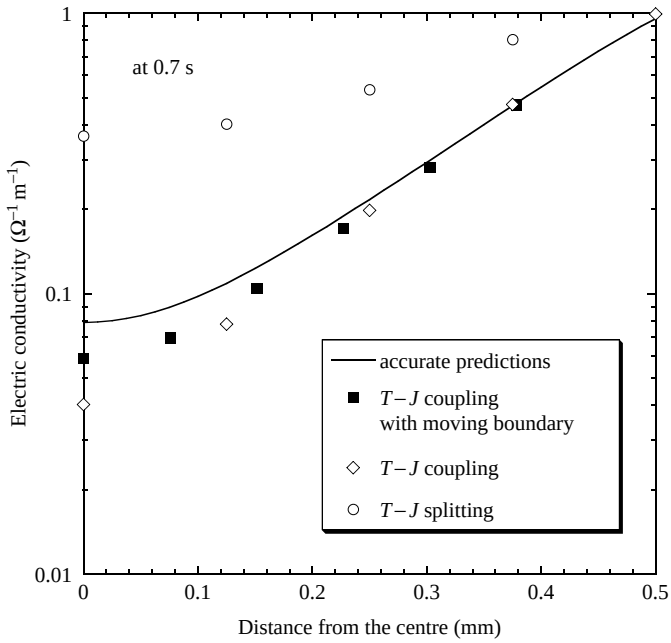

Figure 7.
Numerical predictions of electric conductivity in a thermistor in the middle of the surge stage

Notes: A mesh with 10 space intervals was used and the time step of 20ms was taken. Coupled treatment provides high accuracy

Method	Time step (ms)	Typical iterations numbers per time step at surge (T, ϕ)	Overall T computations	Overall ϕ computations	Overall complexity
Splitting	2	(1, 4-8)	100	340	440
Standard coupling	10	(3-9, 3-14)	106	157	263
Moving coupling	15	(4-11, 5-23)	80	138	218

Table II.
Comparison of computing complexity during 0.6-0.8 s time interval

Notes: The complexity is defined as the total number of matrix inversions at the given time interval. The splitting method utilizes a two-step Runge-Kutta integration and requires two solutions of Poisson equation at each step. To get the matching accuracy (Figure 6), the standard coupling technique should use a smaller time step $\Delta t = 10$ ms as compared with $\Delta t = 15$ ms for the front-fixing method

on each time step, the small time steps become prohibitively expensive. A fully coupled approach on a conventional fixed grid exhibits better performance by a factor of two, while the front-fixing additionally reduces the computational effort by about a quarter.

6. Conclusion

There are several advantages in using a front-fixing method for modelling of non-linear diffusion processes in various electro-magnetic phenomena:

- High accuracy can be achieved on a coarse irregular mesh since the interface is automatically adjusted to crucial regions in new coordinates.

- As a result, larger time steps can be utilised.
- It is useful in handling of strongly non-linear problems, such as encountered in thermistors, high-temperature superconductivity, etc.

The properties of the front-fixing method are such that effective solution algorithms are available:

- Standard high-order monotonic and unconditionally stable schemes for advection problems with diffusion can be used.
- Efficient algorithms for de-coupling of the problem can be implemented.
- Simple iterations converge quickly to provide a self-consistent temperature profile and an interface position.

References

Boris, J.P. and Book, D.L. (1976), "Flux-corrected transport. III. Minimal-error FCT algorithms", *Journal of Computational Physics*, Vol. 20, pp. 397-431.

Carlslaw, H.S. and Jaegar, J.C. (1959), *Conduction of Heat in Solids*, Oxford University Press, Oxford.

Chen, X.F. and Friedman, A. (1993), "The thermistor problem for conductivity which vanishes at large temperature", *Quarterly of Applied Mathematics*, Vol. 51 No. 1, pp. 101-15.

Crank, J. (1984), *Free and Moving Boundary Problems*, Clarendon Press, Oxford.

Fowler, A.C., Frigaard, I. and Howison, S.D. (1992), "Temperature surges in current-limiting circuit devices", *SIAM Journal on Applied Mathematics*, Vol. 52 No. 4, pp. 998-1011.

Golosnoy, I.O. and Sykulski, J.K. (2008), "Evaluation of the front-fixing method capabilities for numerical modelling of field diffusion in high-temperature superconducting tapes", *IET Science, Measurement & Technology*, Vol. 2 No. 6, pp. 418-26.

Illingworth, T.C. and Golosnoy, I.O. (2005), "Numerical Solutions of diffusion-controlled moving boundary problems which conserve solute", *Journal of Computational Physics*, Vol. 209 No. 1, pp. 207-25.

Kutluay, S., Bahadir, R. and Ozdes, A. (1999), "Various methods to the thermistor problem with a bulk electrical conductivity", *International Journal of Numerical Methods in Engineering*, Vol. 45, pp. 1-12.

LeVeque, R.J. (2002), *Finite Volume Methods for Hyperbolic Problems*, Cambridge University Press, Cambridge.

Macklen, E.D. (1979), *Thermistors*, Electrochemical Publications, Ayr.

Platzer, A., Supancic, P. and Danzer, R. (2006), "Thermography and simulation of advanced nonlinear electroceramic components", *Advanced Engineering Materials*, Vol. 8 No. 11, pp. 1134-9.

Preis, K., Biro, O., Supancic, P. and Ticar, I. (2003), "FEM simulation of thermistors including dielectric effects", *IEEE Transactions on Magnetics*, Vol. 39 No. 3, pp. 1733-6.

Preis, K., Biro, O., Dyczij-Edlinger, R., Richter, K.R., Badics, Z., Riedler, H. and Stogner, H. (1994), "Application of FEM to coupled electric, thermal and mechanical problems", *IEEE Transactions on Magnetics*, Vol. 30 No. 5, pp. 3316-9.

Supancic, P. (2000), "Mechanical stability of BaTiO3-based PTC thermistor components: experimental investigation and theoretical modelling", *Journal of the European Ceramic Society*, Vol. 20, pp. 2009-24.

Tannehill, J.C., Anderson, D.A. and Pletcher, R.H. (1997), *Computational Fluid Mechanics and Heat Transfer*, Taylor & Francis, London.

Westbrook, D.R. (1989), "The thermistor: a problem in heat and current flow", *Numerical Methods for PDEs*, Vol. 5, pp. 259-73.

Wood, A.S. and Kutluay, S. (1995), "A heat balance integral model of the thermistor", *International Journal of Heat Mass and Transfer*, Vol. 38 No. 10, pp. 1831-40.

Appendix

Owing to experimental difficulties, a dependence of σ on field E has been measured only for relatively low values $E \leq 1.5$ kV/cm (Supancic, 2000). For $E = 1.5$ kV/cm, it was found that changes in σ are relatively small at room temperature. In contrast, σ increases by an order of magnitude at 160 °C and is approximately doubled at T > 230 °C. At the surge stage, the field E could be significantly higher than 1.5 kV/cm and extrapolation to high E-values is needed. Supancic (2000) suggests a relatively weak dependence on the field:

$$\sigma(T,E) = \sigma(T,0)(1 + const(T)E^2), \tag{A1}$$

whereas another study (Preis *et al.*, 2003) uses a power law:

$$\sigma(T,E) = \sigma(T,0) \cdot 10^{const(T)E}. \tag{A2}$$

There is no strict theoretical justification for equations (A1) or (A2). Moreover, some saturation at large values of E is to be expected. In the paper, it is suggested to develop a uniform interpolation formula which fits into the existing experimental data and also provides gradual saturation of σ for the fields up to $E \sim 5$ kV/cm.

It could be seen from Figure 1 that σ is almost constant for $T < T_1$ and $T > T_2$:

$$\sigma(T \leq T_1, E) \approx \sigma_1(E), \quad \sigma(T \geq T_2, E) \approx \sigma_2(E), \tag{A3}$$

with $\sigma(T \leq T_1, E = 0) \approx 3.33\,\Omega^{-1}\,\mathrm{m}^{-1}$, $\sigma(T \geq T_2, E = 0) \approx 3.33 \cdot 10^{-5}\,\Omega^{-1}\,\mathrm{m}^{-1}$ (Figure 1). It is possible to approximate σ at $T_1 < T < T_2$ using a relatively simple interpolation:

$$\sigma(T,E) \approx \frac{\sigma_1(E)}{B(T,E)}, \tag{A4}$$

with the coefficient B responsible for a smooth transition between σ_1 and σ_2:

$$\log_{10}\ B(T,E) = \frac{1}{2}\log_{10}\left(\frac{\sigma_2(E)}{\sigma_1(E)}\right) \cdot \left(1 + \frac{A_B\zeta(T)}{\sqrt{1 + A_B^2\zeta^2(T)}}\right). \tag{A5}$$

It is assumed that changes in conductivity in the low-temperature phase are negligible, $\sigma_1(E) \approx \sigma_1(0)$. The dependence on the field E in equation (A5) is then taken as:

$$\log_{10}\left(\frac{\sigma_2(E)}{\sigma_1(E)}\right) = \log_{10}\left(\frac{\sigma_2(E=0)}{\sigma_1(E=0)}\right)\left(1 - \frac{A_\sigma|E|}{\left(E^p + E_b^p\right)^{1/p}}\right), \quad E_b = 1.5\,\mathrm{kV\,cm^{-1}}, \tag{A6}$$

and the temperature variation described by $\zeta(T)$:

$$\zeta(T) = \begin{cases} \frac{T-0.5(T_1(E)+T_2(E))}{T_2(E)-T}, 0.5(T_1(E)+T_2(E)) < T < T_2(E) \\ \frac{T-0.5(T_1(E)+T_2(E))}{T-T_1(E)}, T_1(E) < T < 0.5(T_1(E)+T_2(E)) \end{cases} \quad \text{(A7)}$$

with field dependent transition temperatures:

$$T_1(E) = T_1(0) \cdot \left(1 + \frac{A_{1T}|E|}{\left(E^w + E_b^w\right)^{1/w}}\right), \quad \text{(A8)}$$

$$T_2(E) = T_2(0) \cdot \left(1 + \frac{A_{2T}|E|}{\left(E^w + E_b^w\right)^{1/w}}\right). \quad \text{(A9)}$$

The particular choice of numerical coefficients in equations (A5)-(A9) depends on the material itself (mainly on the dopants and the grain structure) and the fitting should be supported by experimental measurements for each individual case. Values of $A_B = 1.5$, $A_\sigma = 0.4$, $A_{1T} = 0.025$, $A_{2T} = 0.1$, $p = 0.5$, $w = 2$ were found to give a good match with experiments (Supancic, 2000; Platzer *et al.*, 2006). In Figure 1, the experimental data (Supancic, 2000) is compared with the interpolation equations (A3)-(A9). It can be seen that the agreement is satisfactory and an increase in the field strength leads to a conductivity rise at high temperatures.

About the authors

Igor O. Golosnoy received his MSc degree in Applied Mathematics and Physics from Moscow Institute of Physics and Technology, Russia in 1992 and the PhD in Mathematics and Physics from Institute for Mathematical Modelling, Moscow, Russia. He is currently a Lecturer at the Electrical Power Engineering Group, School of Electronics and Computer Science, University of Southampton. His research interests include numerical modelling of various coupled electrical, thermal and mechanical phenomena with emphasis on free and moving boundaries problems. Igor O. Golosnoy is the corresponding author and can be contacted at: i.golosnoy@soton.ac.uk; ig@ecs.soton.ac.uk

Jan K. Sykulski is a Professor of Applied Electromagnetics and Head of Electrical Power Engineering at the University of Southampton. His research interests are in the areas of power applications of high-temperature superconductivity, modelling of superconducting materials, advances in simulation of coupled field systems (electromagnetic, circuits and motion), development of fundamental methods of computational electromagnetics and new concepts in design and optimisation of electromechanical devices. He has over 270 publications listed on the official database of the University. He is a Founding Member and Chair of the Professional Network Electromagnetics of IET, a Founding Secretary/Treasurer/Editor of International Compumag Society, a visiting professor at universities in Canada, France, Italy, Poland and China and a member of International Steering Committees of major international conferences, including COMPUMAG, IEEE CEFC, IEE CEM, EMF, ISEF, EPNC, ICEF and others. He is a Fellow of IEE, Institute of Physics and British Computer Society and has an honorary title of Professor awarded by the President of Poland.